

A COMPARATIVE STUDY OF COMPOSITE MODELLING APPROACHES USED FOR THERMO-STAMPING PROCESS

Halil Yildirim¹
Ankara Yildirim Beyazit University
Ankara, Turkey

Prof. Dr. Fahrettin Ozturk²
Ankara Yildirim Beyazit University
Ankara, Turkey

ABSTRACT

Two approaches are commonly used in composite modelling; namely one shell element (OSE) model and multi-elements (ME) model. In this study, although the ME model is a more accurate approach to capture the interaction between the plies of multi-layered composites in the simulation of the thermo-stamping process, it is investigated whether acceptable results can be obtained by using the OSE model, which is a computationally efficient model for composite modeling. Simulation results show that as the relative angle of the fibers between neighboring plies increases, the results obtained with the OSE model leads to unrealistic results.

INTRODUCTION

The use of thermoplastic composites in the aerospace industry has gradually increased in recent years. Thermoplastic composites have significant advantages during fabrication. One of its main advantages is to allow the application of thermo-stamping which is a popular processing technique because of the fast cycle time, allowing production at low cost (Vanclouster, 2010). Woven fabrics are generally used as reinforcement elements in the manufacturing doubly curved parts with the thermo-stamping method due to their better formability properties than unidirectional reinforcement elements (Peng & Ding, 2011). The thermo-stamping method consists of three stages: First, the laminate, which is formed by stacking the flat prepreg layers on top of each other, is transferred to the mold after heating it to a temperature higher than the melting temperature of the matrix by a heater. Second, by moving the upper or lower mold through a press, the two molds close onto each other. Third, pressure is applied to the formed part for a while and the laminate is waits for cooling and hardening between the molds. The pressure applied at the last stage is for the resin to penetrate the cavities better and to achieve a better interlaminar adhesion (Willems, 2008).

Wrinkle formation is the most common problem encountered in the thermo-stamping process of doubly curved parts. The wrinkling behavior of single dry fabrics has been studied numerically and experimentally in many studies, among which it has been revealed that the most effective parameter in wrinkle formation is the shear locking angle (Owlia, Najjar, & Taviana, 2020; Gherissi et al., 2016; Boisse et al., 2011; Rashidi & Milani, 2018; Allaoui et al.,

¹ Ph.D Student, Department of Mechanical Engineering, Email: hyildirim@ybu.edu.tr

² Professor, Department of Mechanical Engineering, Email: fozturk@ybu.edu.tr

2011). Wang et al. (Wang et al., 2014) have shown that the forming temperature is effective on wrinkle formation in thermo-stamping processes of prepregs. In the industry, thermo-stamping is mostly applied to multi-layered composites and the deformation mechanisms of multi-layered composites are different from those of single-layered composites. Vanclooster (Vanclooster, 2010) demonstrated the relationship between wrinkle formation and relative ply orientation in multi-layered composites. Guzman-Maldonado et al. (Guzman-Maldonado et al., 2019) investigated both experimentally and numerically the effect of ply orientation, inter-ply friction, blank holder pressure on wrinkle formation in multi-layered composites during the thermo-stamping process.

Finite element analysis (FEA) is an efficient method at the design stage of composite parts since the application of trial and error methods to estimate the possible defects is often expensive and time-consuming. Two approaches are common in composite modelling: The first approach models the multi-layered composite using one shell element for all the layers. This approach is named as one shell element (OSE) model in this paper. OSE model does not consider the inter-ply slippage behavior of the composite, and therefore it is unsuitable for thermo-stamping simulation of multi-layered composites. However, it is computationally efficient and it can be used for cases where inter-ply slippage can be neglected. The second approach is based on modelling the layers individually. This approach is named as multi-elements (ME) model in this paper. Even though ME model considers inter-ply slipping behavior and frictional interactions between layers in the thermo-stamping process, it is computationally quite expensive since the number of elements and contact definitions increase according to the number of layers. This study compares two methods in modelling the thermo-stamping of multilayered composites.

METHOD

Finite Element Modelling

A plain woven thermoplastic composite (glass fiber and PPS resin) is used in composite laminate for this study. The mechanical properties of the E-glass fabric reinforcement are taken from the literature (Mohammed, Lekakou, & Bader, 2000). Analysis are carried out using three different lay-ups: $[0/90]_2$, $[0/90,-15/75]$, and $[0/90,-45/45]$. The square-shaped composites have a dimension of 320x320 mm. 194 mm diameter hemispherical punch is used in the simulations since it is the simplest geometry representing the double curvature geometry. The diameter of blank holder and die cavities is 200 mm. The schematic of the thermo-stamping set-up and one-quarter model used in the simulations are displayed in Figure 1. Thermo-stamping process is simulated using the commercial FE software LS-DYNA. MAT_REINFORCED_THERMOPLASTIC (MAT_249) material model is used to describe the woven fabric reinforced thermoplastic behavior. The analysis is carried out under the assumption of constant temperature during the forming process. Therefore, the mechanical properties of PPS at 300 °C is defined in the material card.

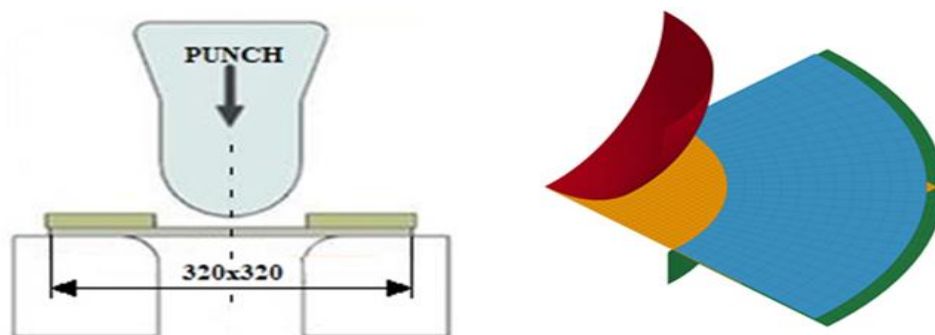


Figure 1: The geometry and the simulation model of the tools

The simulation model includes four parts: hemispherical punch, the blank holder, die, and woven fabric reinforced thermoplastic composite. Rigid shell elements are assigned for the tools while the composite is modelled as deformable shell elements. A total of 1600 shell elements are used in OSE model while 3200 shell elements (1600 shell elements for each layer) are used in ME model. While tool-to-ply friction coefficient is assumed to be 0.21 in both OSE and ME models, ply-to-ply friction coefficient is assumed as 0.23 in ME model based on the literature (Guzman-Maldonado et al., 2019). Contact definition between the tool and the composite is forming_surface_to_surface in both model while ply-to-ply contact is defined as tiebreak contact in ME model. The blank holder applies a constant force of 2 kN during the process.

RESULTS

Thermo-stamping simulation for all 3 lay-ups is performed using both OSE and ME models. Figure 2 shows the deformed shape and shear angle contour maps obtained in 60 mm punch stroke in the simulation performed with both models for $[0/90]_2$ orientation. In the analysis performed using a computer with Intel (R) Core (TM) i7-4500U CPU, the solution time is approximately 4 minutes and 11 minutes for the OSE and ME models, respectively, demonstrating that OSE model is computationally much more efficient than the ME model.

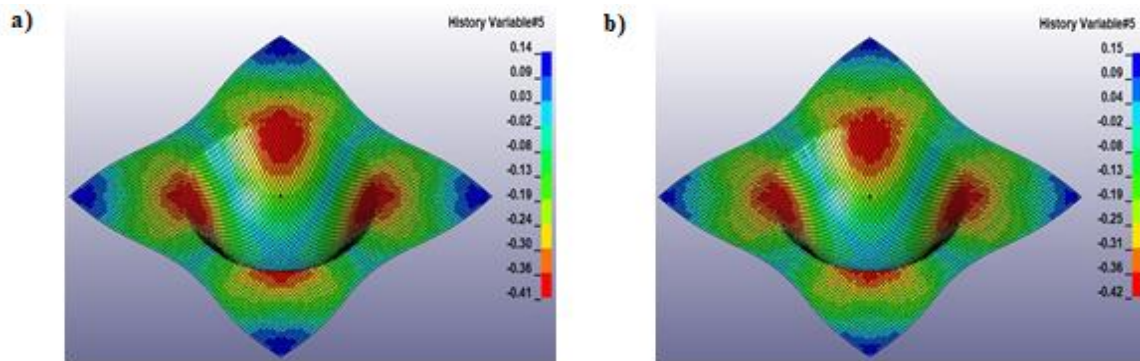


Figure 2: Shear angle contour maps of the top layers for $[0/90]_2$ lay-up: a) OSE model results b) ME model results

The contour maps given in Figure 2 only show the shear angle distribution of the top layers. Since no difference is observed in both models between the shear angle distribution of the bottom and the top layer for $[0/90]_2$ lay-up, the shear angle contour maps of the bottom layer is not included in the paper. As seen in Figure 2, no wrinkle formation is observed in both models. The contour maps of both models show that the shear angle distribution of the deformed composite is very close to each other. While the maximum shear angle is obtained as 0.41 rad in the OSE model, 0.42 rad is obtained in the ME model.

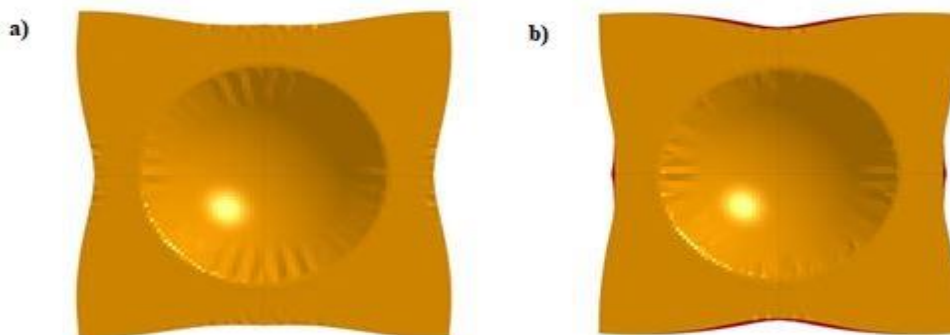


Figure 3: Wrinkles on deformed composite laminate with $[0/90,-15/75]$ lay-up: a) OSE model results b) ME model results

Figure 3 demonstrates the deformed $[0/90,-15/75]$ laminates obtained by both models. While a small amount of wrinkle formation is predicted on the deformed laminate in both models, it is seen that the wrinkles are more pronounced according to the estimation obtained from the OSE model. Besides, there is some difference in the estimation of the boundary profile of both models. The appearance of the red-colored outer layer from the edges in the OSE model indicates that there is a small amount of inter-ply slippage.

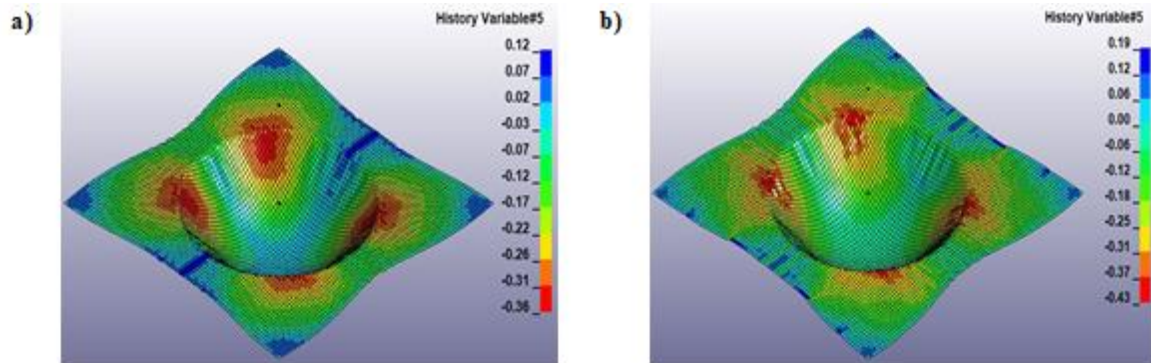


Figure 4: Shear angle contour maps of the top layers for $[0/90,-15/75]$ lay-up: a) OSE model results b) ME model results

Figure 4 demonstrates the shear angle distribution of the top layers for $[0/90,-15/75]$ lay-up obtained by both models. Although the shear angle distributions obtained from the two models are similar, it is clear that there is some difference. The maximum shear angle is estimated by the OSE and ME models as 0.36 rad and 0.43 rad, respectively. When the shear angle contour maps obtained for the top layers are examined, it is seen that the maximum shear deformation region obtained with the ME model covers a smaller area than that of the OSE model.

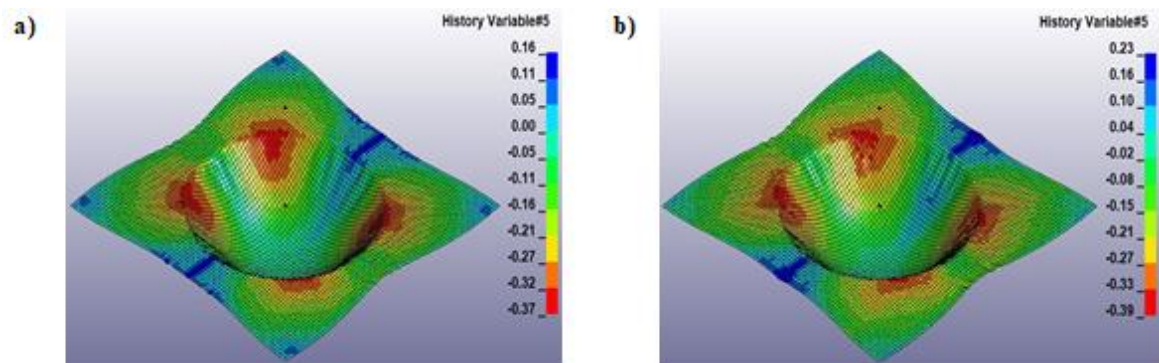


Figure 5: Shear angle contour maps of the bottom layers for $[0/90,-15/75]$ lay-up: a) OSE model results b) ME model results

The shear angle contour maps of the bottom layer obtained with both models are quite compatible with each other, as seen in Figure 5. The maximum shear angle is estimated by the OSE and ME models as 0.37 rad and 0.39 rad, respectively. If the top layer and bottom layer are compared, it is seen that the difference between the maximum shear angles in the ME model results is greater than that in the other model. This difference can be explained by the inter-ply slippage effect.

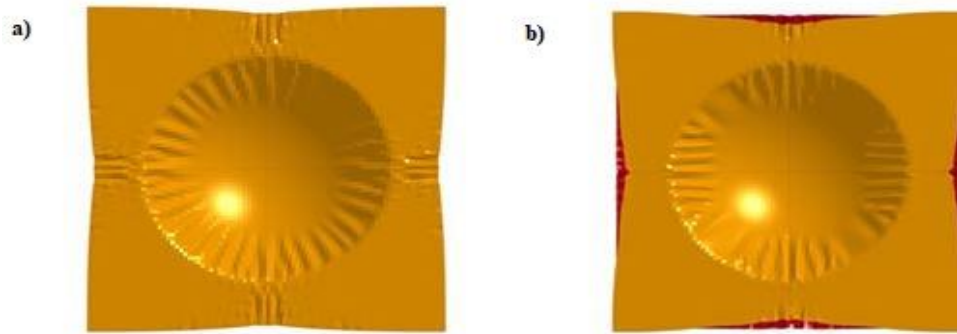


Figure 6: Wrinkles on deformed composite laminate with $[0/90,-45/45]$ lay-up: a) OSE model results b) ME model results

The analysis is finally applied for $[0/90,-45/45]$ laminate. As seen in Figure 6, it is observed that the amount and size of wrinkles increase compared to other laminates. When the results obtained with both models are examined, it is seen that more wrinkles occur on the deformed composite as a result of the analysis performed with the OSE model, and the wrinkles formed are larger than the other model. It can also be concluded that as the relative orientation between adjacent plies increases, the divergence between the wrinkle predictions of the two models increases. As seen in Figure 6 b), the red outer ply protrudes from the edges more than $[0/90,-15/75]$ laminate previously analyzed. This shows that as the relative orientation between adjacent plies increases, inter-ply slippage increases.

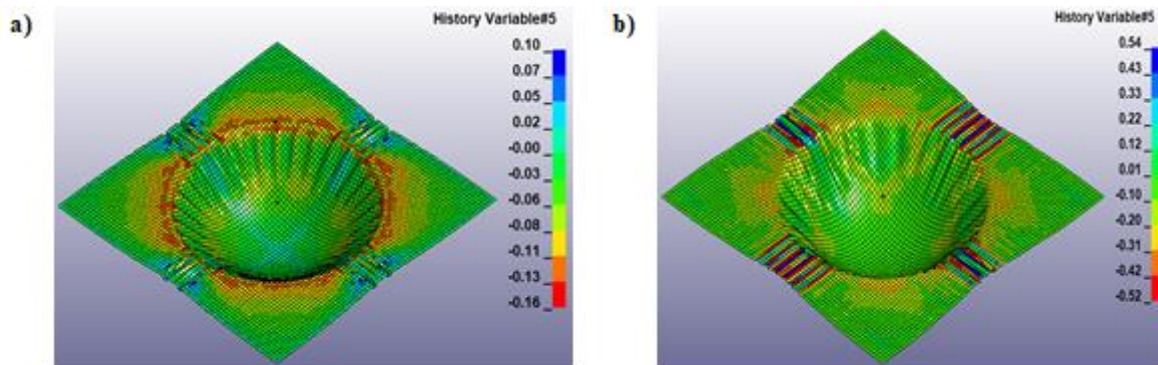


Figure 7: Shear angle contour maps of the top layers for $[0/90,-45/45]$ lay-up: a) OSE model results b) ME model results

Figure 7 demonstrates the shear angle distribution of the top layers for $[0/90,-45/45]$ lay-up obtained by both models. A large deviation is seen between the shear angle estimation of the two models. The maximum shear angle in the top layer is estimated by the OSE and ME models as 0.16 rad and 0.52 rad, respectively. In both models, maximum shear deformations occur on the flange region where the blank holder contacts. Maximum shear deformations do not gather in a certain region and have a scattered appearance. It is noteworthy that maximum shear deformations occur in the flange region.

The maximum shear angle in the bottom layer is estimated by the OSE and ME models as 0.33 rad and 0.37 rad, respectively. When the shear angle contour maps of the bottom layer are examined in Figure 8, it can be noticed that the shear angle distribution is quite different from that of the top layer, such that even though shear deformations in the bottom layer occur in the flange region as in the case of top layer, however, since the wrinkles in the flange region are less in the bottom layer than in the top layer, the maximum shear deformation zones are not scattered in the bottom layer as in the top layer.

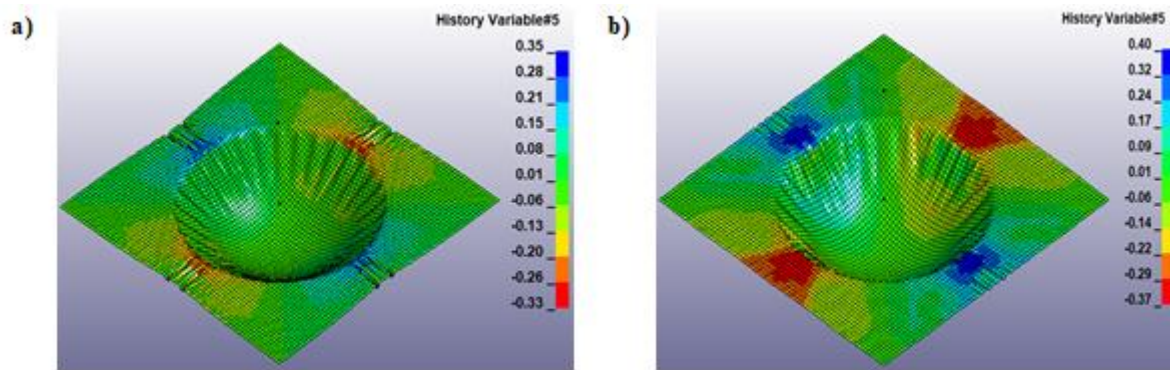


Figure 8: Shear angle contour maps of the bottom layers for [0/90,-45/45] lay-up: a) OSE model results b) ME model results

Table 1 contains the predictions of the maximum shear angles obtained by the OSE and ME models in the bottom and top layer for three different lay-ups. It is seen that the maximum shear angle values obtained with the OSE model for both layers are lower than the ME model predictions. In addition, as the angular orientation difference between the layers increases, the deviation in the predictions of both models gradually increases. Since the OSE model does not allow inter-ply slippage, intra-ply shearing is restricted during deformation. Therefore, the OSE model underestimates the maximum shear angle.

Table 1: Maximum shear angle predictions of the models

	[0/90] ₂ lay-up	[0/90,-15/75] lay-up	[0/90,-45/45] lay-up
OSE model (Top layer)	0.41 rad	0.36 rad	0.16 rad
ME model (Top layer)	0.42 rad	0.43 rad	0.52 rad
OSE model (Bottom layer)	0.41 rad	0.37 rad	0.33 rad
ME model (Bottom layer)	0.42 rad	0.39 rad	0.37 rad

CONCLUSION

Thermo-stamping simulations of multi-layered thermoplastic composites consisting of two fabric-reinforced laminae with the different orientations are performed using two different composite modelling approaches called OSE and ME model. Both models show similar results for the [0/90]₂ oriented composite in terms of wrinkling behavior and shear angle distribution. As the relative angle of the fibers between neighboring plies increases, the results obtained with the OSE model show more wrinkle formation. Therefore, the OSE model, which significantly decreases the solution time in the simulation of the thermoforming process of composites with low relative orientation between plies, can be preferred since it will give acceptable results.

References

Allaoui, S., Boisse, P., Chatel, S., Hamila, N., Hivet, G., Soulat, D., & Vidal-Salle, E. (2011). Experimental and numerical analyses of textile reinforcement forming of a tetrahedral shape. *Composites: Part A*, Vol. 42, p: 612-622.

- Boisse, P., Hamila, N., Vidal-Salle, E., & Dumont, F. (2011). Simulation of wrinkling during textile composite reinforcement forming. Influence of tensile, in-plane shear and bending stiffnesses. *Composites Science and Technology*, Vol. 71, p: 683-692.
- Gherissi, A., Abbassi, F., Ammar, A., & Zghal, A. (2016). Numerical and experimental investigations on deep drawing of G1151 carbon fiber woven composites. *Applied Composite Materials*, Vol. 23, p: 461-476.
- Guzman-Maldonado, E., Wang, P., Hamila, N., & Boisse, P. (2019). Experimental and numerical analysis of wrinkling during forming of multilayered textile composites. *Composite Structures*, Vol. 208, p: 213-223.
- Mohammed, U., Lekakou, C., & Bader, M.G. (2000). Experimental studies and analysis of the draping of woven fabrics. *Composites: Part A*, Vol. 31, p: 1409-1420.
- Owlia, E., Najjar, S.S., & Tavana, R. (2020). *Experimental and macro finite element modeling studies on conformability behavior of woven nylon 66 composite reinforcement*. *The Journal of the Textile Institute*, Vol. 111, p: 874-881.
- Peng, X., & Ding, F. (2011). Validation of a non-orthogonal constitutive model for woven composite fabrics via hemispherical stamping simulation. *Composites: Part A*, Vol. 42, p: 400-407.
- Rashidi, A., & Milani, A.S. (2018). *Passive control of wrinkles in woven fabric preforms using a geometrical modification of blank holders*. *Composites: Part A*, Vol. 105, p: 300-309.
- Vanclooster, K. (2010). Forming of multilayered fabric reinforced thermoplastic composites. Ph.D. Thesis, Katholieke Universiteit Leuven, Leuven.
- Wang, P., Hamila, N., Pineau, P., & Boisse, P. (2014). Thermomechanical analysis of thermoplastic composite prepregs using bias-extension test. *Journal of Thermoplastic Composite Materials*, Vol. 27, p: 679-698.
- Willems, A., (2008). *Forming simulation of textile reinforced composite shell structures*. Ph.D. Thesis, Katholieke Universiteit Leuven, Leuven.